Nano Research 2015, 8(10): 3197–3204
DOI 10.1007/s12274-015-0819-6
Research Article
ISSN 1998-0124
CN 11-5974/O4

Cylindrical spiral triboelectric nanogenerator

Xiao Hui Li[1,§], Chang Bao Han[1,§], Li Min Zhang[1], and Zhong Lin Wang[1,2] (✉)

[1] *Beijing Institute of Nanoenergy and Nanosystems, Chinese Academy of Sciences, Beijing 100083, China*
[2] *School of Material Science and Engineering, Georgia Institute of Technology, Atlanta, Georgia 30332, USA*
[§] *These authors contributed equally to this work.*

Received: 12 March 2015
Revised: 14 May 2015
Accepted: 18 May 2015

KEYWORDS
triboelectric nanogenerator, self-powering, displacement sensor

ABSTRACT

In recent years, triboelectric nanogenerators have attracted much attention because of their unique potential in self-powered nanosensors and nanosystems. In this paper, we report a cylindrical spiral triboelectric nanogenerator (S-TENG), which not only can produce high electric output to power display devices, but also can be used as a self-powered displacement sensor integrated on a measurement ruler. At a sliding speed of 2.5 m/s, S-TENG can generate a short-circuit current (I_{SC}) of 30 μA and an open-circuit voltage (V_{OC}) of 40 V. As the power source, we fabricate a transparent and flexible hand-driven S-TENG. Furthermore, we demonstrate a self-powered S-TENG-based measuring tapeline that can accurately measure and display the pulled-out distance without the need for an extra battery. The results obtained indicate that TENG-based devices have good potential for application in self-powered measurement systems.

1 Introduction

Portability, which enables a more convenient and simple lifestyle, has attracted increasing attention [1, 2]. Portable devices such as mobile phones, digital cameras, MP3/MP4 players, navigation systems, and E-books play a vital part in our contemporary society because they can fulfill a variety of functions that meet our daily needs. However, an obvious problem is that those conventional devices usually rely on batteries that need to be recharged or replaced because of their limited lifetime. Therefore, to reduce the dependence on external power sources that hinder the further development of portable devices, we propose a self-powered system that harvests energy from ambient environment. To date, many self-powered devices based on solar cells [3], piezoelectrics [4–6], pyroelectrics [7–9], and electromagnetics [10, 11], have been fabricated, and several forms of energies have been transformed into electricity.

Recently, a triboelectric nanogenerator (TENG), that focuses on the universally existing mechanical motion, has been demonstrated as a promising way to directly convert ambient mechanical energy into electricity [12–15]. Previous studies have shown that slight movements can be easily transformed into significant electrical signals using TENG technology, which provides an excellent way for self-powered displacement

Address correspondence to zlwang@gatech.edu

sensors [16–18]. At the same time, the constant motion will generate a high electric output that can also meet the needs of electricity for portable devices. Consequently, we can choose appropriate materials, structures, and designs to achieve a high output for self-powered sensors and electronics. In previous studies, several novel structures such as grid configurations, tube structure, and flexible design have been fabricated to realize sensor functions [19–21].

In this study, we designed a cylindrical spiral triboelectric nanogenerator (S-TENG) to realize a high space utilization and self-powered tapeline display. Based on the vertical contact-separation mode, the S-TENG can deliver an open-circuit voltage (V_{OC}) of ~ 40 V and a short-circuit current density (J_{SC}) of ~2.5 mA/m^2 at an acceleration of 25 m/s^2. We prepared a flexible and transparent S-TENG with a V_{OC} of ~250 V and transferred charge quantity (ΔQ) of 2.5 μC, which can simultaneously light up about 100 commercial light-emitting diode (LED) bulbs. Furthermore, we fabricated a self-powered measuring tapeline based on the S-TENG structure and its output V_{OC} has a nearly linear relationship with the sliding displacement, which can simultaneously realize the self-powered measurement and display.

2 Experimental section

2.1 Fabrication of the S-TENG

The fabrication of the S-TENG started from Kapton films (0.1-mm thickness) that were cleaned with alcohol, acetone, and deionized water in sequence, then heated in an oven at 60 ℃ to evaporate the water. Next, we deposited a layer of 100-nm copper on one side of the Kapton film. Then, we cut commercial Al films, PET films, and Kapton films into the same size (15 mm × 180 mm). Those films were then stacked layer-by-layer, curled up, and heated in the oven at 70 ℃ to maintain their spiral structure, with Kapton and Al layers serving as the friction area, as shown in Fig. 1(a). The S-TENG was driven by a linear motor (Linmot E1100), while the transferred charge and V_{OC} were measured by an electrometer (Keithley, 6514). We measured the short-circuit current of the S-TENG using a Stanford low-noise current preamplifier (Model SR570).

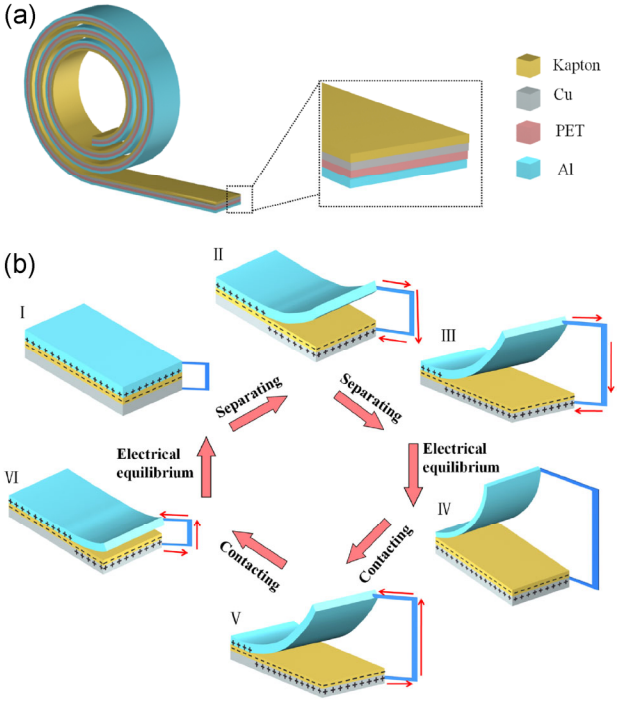

Figure 1 Working mechanism of the S-TENG. (a) Schematic of the basic structure of the S-TENG. (b) Description of the TENG's working mechanism.

2.2 Fabrication of the hand-driven S-TENG

We cut the commercial polyethylene terephthalate (PET) films into the size of 100 mm × 180 mm, after which we placed two parallel TENGs at the top and bottom of the PET film. Each TENG has the same contact area of 15 mm × 180 mm.

2.3 Fabrication of the self-powered measuring tapeline

We fabricated the S-TENG into a tapeline and a liquid crystal display (LCD) screen was connected to an external circuit to show the pulled-out displacement without any extra power sources. Then, we applied the grating-structured Kapton films to the tapeline, and a Cu cylindrical roller was fixed at the edge of the tapeline. The close contact between the grating-structured Kapton and Cu roller results in corresponding current output signals, which was also measured using a Standford low-noise current preamplifier (Model SR570).

3 Result and discussion

The structure of the S-TENG is depicted in Fig. 1(a).

The planar TENG consists mainly of four layers: Kapton (friction material), Cu (electrode), PET (insulator), and Al (friction and electrode), and it was then curled up and heated in the oven at 70 ℃ to maintain its spiral structure. We chose Kapton and Al as friction materials because of their high electrification during contact. The working principle of the S-TENG is demonstrated in Fig. 1(b). In the original position, we assume that the Kapton and aluminum film are in full contact with each other. Because Kapton is more triboelectrically negative than Al, it is easy to have negative charges on the surface, while Al will have an equal amount of positive charges on the surface. Therefore, there is no charge flowing in the external circuit because of the electrostatic equilibrium. When the Al film is separated from the Kapton film, an electric potential drop is generated and drives the positive charge flow from the top Al electrode to the bottom Cu electrode. This produces a transient current in the external circuit. Once the Al film is fully separated from the Kapton film, all of the positive charges are transferred to the Cu electrode, with another electrostatic equilibrium being reached. Subsequently, when the Al film moves back, the positive charge flow is reversed, generating another external-circuit current in the opposite direction. Therefore, a periodic alternating current (AC) output can be produced during the cyclic motion of the device.

According to the mechanism of the in-plane structured TENG [22, 23], the theoretical short-circuit current (I_{SC}) of a conductor-to-dielectric contact-separation mode for the sliding-mode TENG is given by

$$I_{SC} = \frac{\Delta Q}{\Delta t} = \frac{\sigma w \Delta x}{\Delta t} = \sigma w v \quad (1)$$

where σ is a constant value representing the transferred charge density, Δx is the pulled-out displacement, v is the velocity of TENG during the cyclic motion, and w is the width of the Kapton film. Here, Eq. (1) approximately matches S-TENG. As a result, the current output is proportional to the speed of the pulled-out displacement.

We measured the output performance of S-TENG using a linear motor (Linmot, E1100). At a symmetric acceleration of 25 m/s^2 and a maximum speed of 2 m/s, V_{OC} and I_{SC} can reach 30 V and 15 μA (Figs. 2(a) and 2(b), respectively). The relationship between the output current/voltage with the velocity and acceleration is shown in Figs. 2(c) and 2(d), respectively. We find that V_{OC} remains mostly unchanged, and as the velocity increases, I_{SC} approximately linearly, and is nearly in accordance with Eq. (1). However, the linearity is not

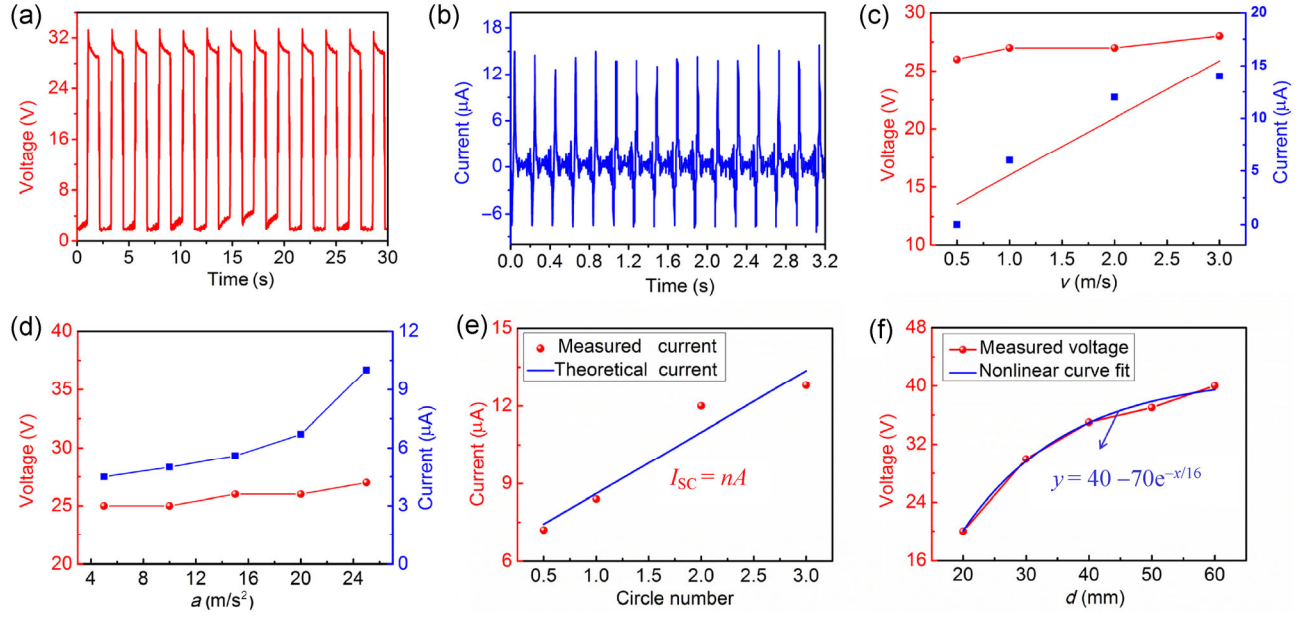

Figure 2 Measurement of the TENG's output. (a) Open-circuit voltage (V_{OC}). (b) Short-circuit current (I_{SC}). (c) The relationship between the output current/voltage and the velocity. (d) The relationship between the output current/voltage and the acceleration. (e) The relationship between the output current and the number of laps. (f) The relationship between the voltages and displacement.

very good because of the uneven distribution of the triboelectric charge density (σ) on the curved surface and non-full contact between the Al and Kapton films during the circular motion. Similarly, V_{OC} remains almost the same, while I_{SC} increases slowly with increasing acceleration. Figure 2(e) illustrates a linear relationship between the output current and the circle number. Theoretically, a larger circle number results in a greater contact area, thus leading to a larger current output, which is close to theoretical speculation. Besides, we also investigated the relationship between V_{OC} and the pulled-out displacement, as shown in Fig. 2(f), the measured output voltage increases with different displacement (20, 30, 40, 50, and 60 mm), which largely conforms to exponential growth.

When we combine this S-TENG with the large area of the transparent and flexible PET film, we can fabricate a hand-driven curly TENG, as shown in Figs. 3(a) and 3(b). The model presented here has two parallel TENGs at the top and bottom PET film, and each TENG has the same friction area of 15 mm × 180 mm. When the TENG is driven manually, the Kapton and Al films will have relative motion, and once the Kapton and Al films make contact with each other, they will glide in opposite directions and return to the initial curved state when they are let go. Thus, an AC current is produced by harvesting the mechanical energy produced during the cyclic movement, and the relevant maximum I_{SC}, V_{OC}, and transferred charge quantity (ΔQ) are 20 μA, 250 V, and 2.5 μC, respectively (Figs. 3(c)–3(e)). With such excellent output performance, this hand-driven TENG can simultaneously

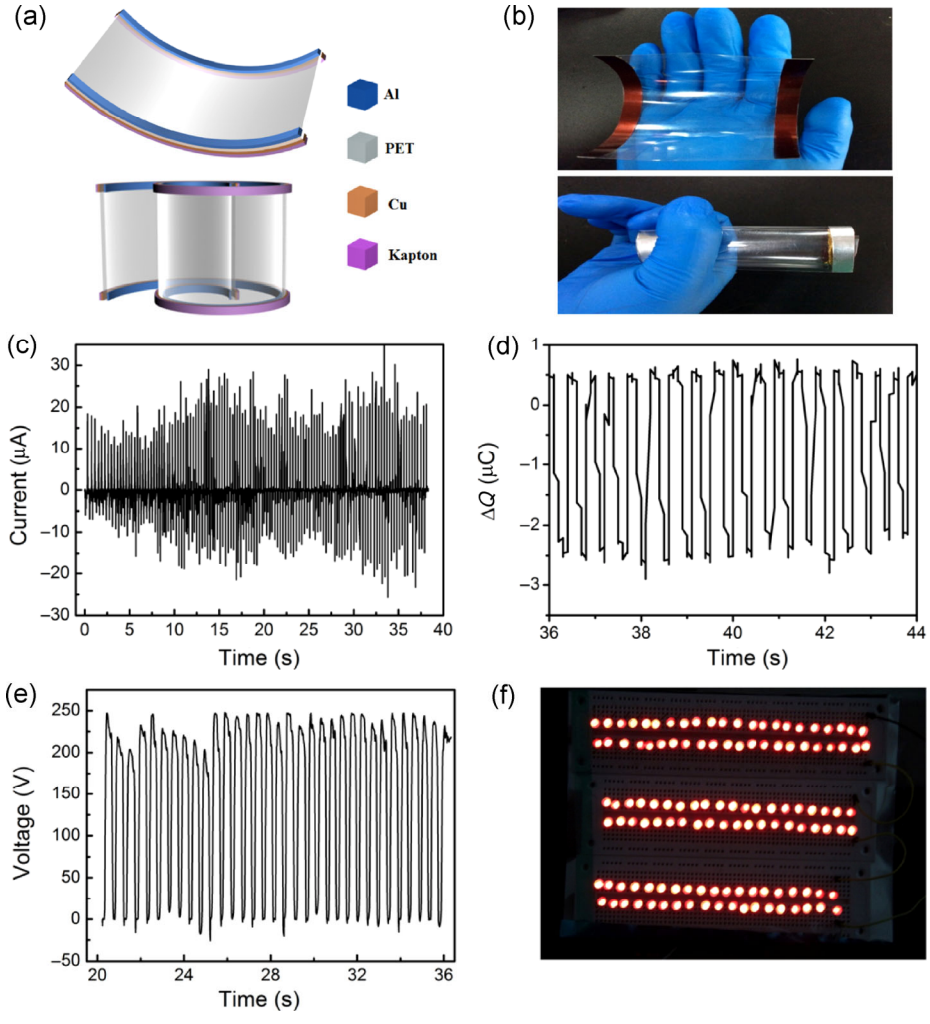

Figure 3 (a) The structure and (b) photograph of hand-driven S-TENG. (c) Short-circuit current. (d) Open-circuit voltage. (e) Transferred charge quantity (ΔQ). (f) Illumination of 100 LEDs using a hand-driven S-TENG with a size of 15 mm × 180 mm.

light up about 100 red LED bulbs (Fig. 3(f)). With a high output, the TENG is shown to be promising for direct use as a power source to drive continuum-electricity-consuming personal electric devices.

Furthermore, when applying this S-TENG to the measuring tapeline, which is a common device in our daily life, we can obtain a self-powered and distance-measuring tapeline without the need for an additional extra battery. The structure of the tapeline is shown in Fig. 4(a). We used Kapton and Al films with an area of 15 mm × 180 mm as the friction materials. When the films are pulled out, an electric output will be produced to power an external screen displaying corresponding distance (Fig. 4(b)). In addition, we systematically investigated the relationship between the output of the self-powered tapeline and the displacement, as shown in Fig. 4(c). It is obvious that the output of the TENG effectively increases with the increase of displacement. The voltage increases from 4 to 17 V when the displacement increases from 1 to 8 cm. Theoretically, the relationship between V_{OC} and the displacement conforms to a linear increase because a larger contact area can be created with a longer displacement. Hence, when we extract the voltage values from Fig. 4(c) and plot them in Fig. 4(d), we observe an approximately linear relationship between the open-circuit voltage and the pulled-out displacement. However, the linearity is not very good, especially when the displacement increases from 2 to 4 cm. This may be due to the non-full contact and internal resistance during the pulled-out motion.

In order to further optimize the output performance of the tapeline when measuring the pulled-out displacement, we introduced the grating structure to S-TENG, as shown in Figs. 5(a) and 5(b). We divided the Kapton film into a series of uniform stripes, and each stripe is 5 mm in width and has an interval separation of 5 mm with each other. We placed a small 8-mm diameter cylindrical roller covered with Cu film at the edge of the tapeline. As a result, we can obtain two generators in the entire tapeline. One is made up of the Al electrode and Cu electrode, which will supply the power to the LCD screen, and the other one consists of the Cu electrode and Cu pillar, giving the current signs to measure the pull-out distance. When we pulled out the films, the Cu pillar will make contact with the Kapton stripes one-by-one, and we recorded corresponding current signals using anSR570 low-noise current amplifier (Stanford Research System). Once the Cu pillar sweeps over an entire Kapton stripe, there will be a positive and a negative current peak in the current graph, which represents a moving distance of 10 mm. In this way, we can determine the moving distance from the number of positive or negative peaks. Further, a detailed description of the TENG's working mechanism is

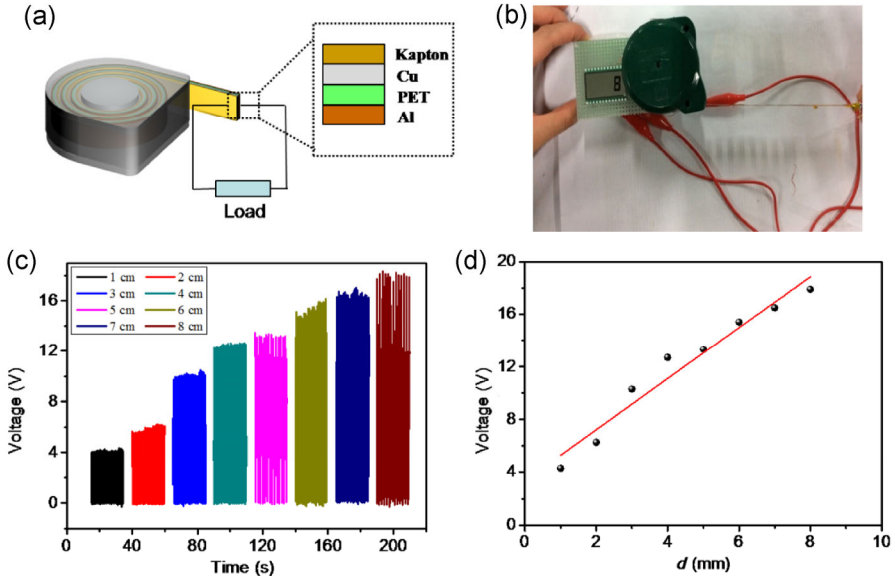

Figure 4 (a) The structure and (b) picture of a self-powered tapeline. (c) The relevant output voltage with different displacements. (d) The measured relationship between the output voltages and the displacements.

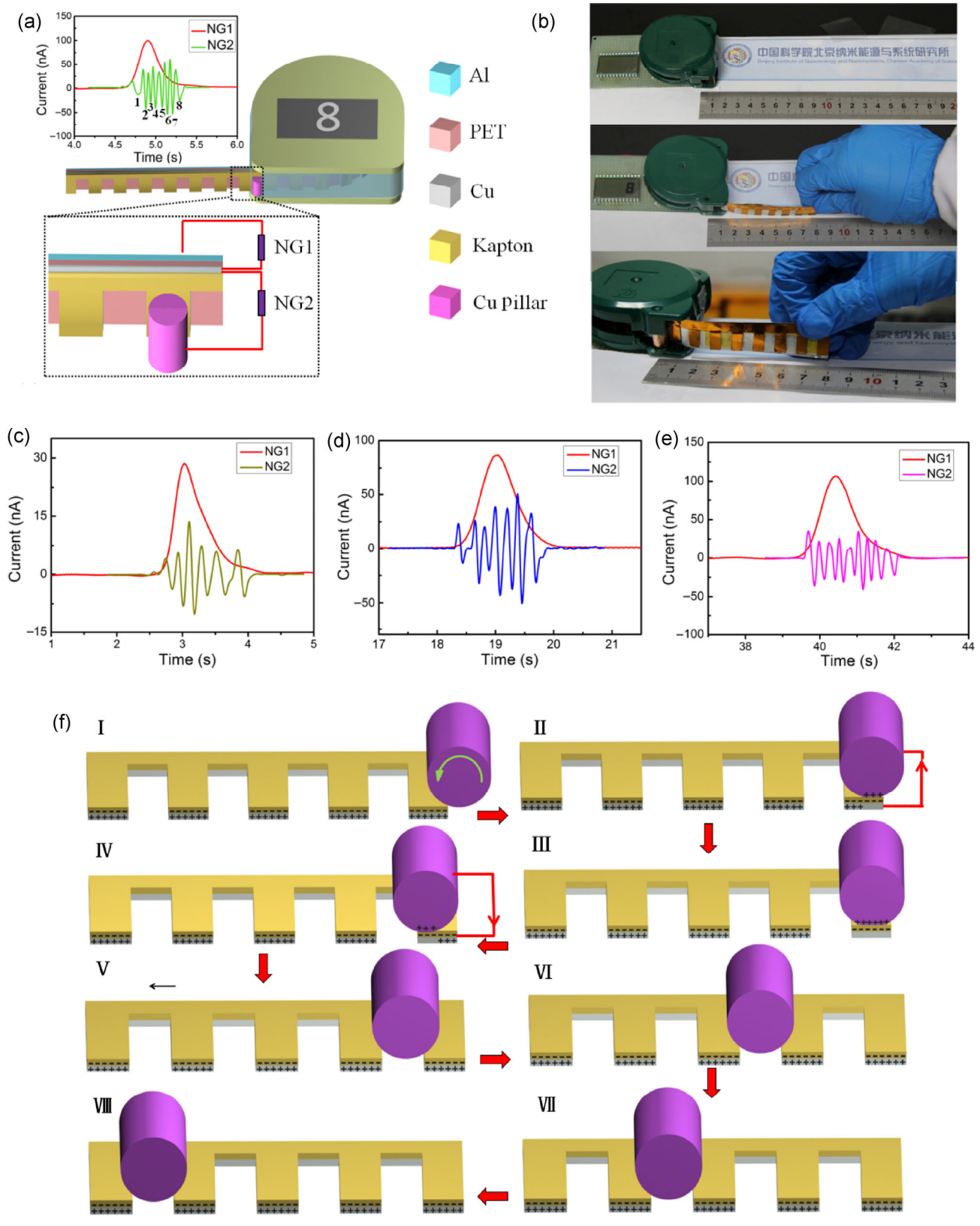

Figure 5 (a) The structure and (b) picture of self-powered grating tapeline. (c)–(e) The output current with different displacements of 6, 7, and 9 cm, respectively. (f) The description of the TENG's working mechanism.

shown in Fig. 5(f). Figures 5(c)–5(e) are current signs at different moving displacements of 6, 7, and 9 cm, respectively, and we observe that the grating-structure tapeline can accurately measure the pulled-out distance.

4 Conclusion

In summary, we have demonstrated a new spiral-shaped TENG structure that is based on contact-separation electrification. By directly converting the mechanical energy to electricity in the separating motion, the S-TENG can generate a short-circuit current (I_{SC}) of 30 μA and an open-circuit voltage (V_{OC}) of 40 V with a maximum short-circuit current density (J_{SC}), acceleration, and speed of ~2.5 mA/m^2, 25 m/s^2, and 2.5 m/s, respectively. We obtained a linear relationship between I_{SC} and the velocity, but V_{OC} increases exponentially with displacement. We prepared a transparent and flexible hand-driven S-TENG, and the maximum I_{SC}, open-circuit V_{OC} and transferred charge quantity (ΔQ) produced by this device reached 20 μA, 250 V, and 2.5 μC, respectively. With such excellent output performance, this hand-driven TENG can instantaneously light up about 100 red LEDs bulbs. For practical applications, we fabricated an S-TENG combined with the measuring tapeline to form a self-powered and distance-measuring tapeline without an external power source. In addition, by comparing the peak numbers in the current signs with the moving displacement, we confirmed that the use of the grating structures was an effective method of realizing a self-powered distance-measuring tapeline with high sensitivity. Thus, this new cylindrical spiral TENG establishes a new field of self-powered devices that may have more practical applications in the harvesting of mechanical energy from our ambient environment.

Acknowledgements

Thanks for the support from the "thousands talents" program for pioneer researcher and his innovation team, China, National Natural Science Foundation of China (Nos. 51432005 and 61405131), Beijing Natural Science Foundation (No. 4154090), Beijing City Committee of science and technology (Nos. Z131100006013004 and Z131100006013005).

Electronic Supplementary Material: Supplementary material (Video S1 demonstrates the effects of the hand-driven S-TENG discussed in the text) is available in the online version of this article at http://dx.doi.org/10.1007/s12274-015-0819-6.

References

[1] Patolsky, F.; Timko, B. P.; Yu, G. H.; Fang, Y.; Greytak, A. B.; Zheng, G. F.; Lieber, C. M. Detection, stimulation, and inhibition of neuronal signals with high-density nanowire transistor arrays. *Science* **2006**, *313*, 1100–1104.

[2] Tarascon, J. M.; Armand, M. Issues and challenges facing rechargeable lithium batteries. *Nature* **2001**, *414*, 359–367.

[3] Huynh, W. U.; Dittmer, J. J.; Alivisatos, A. P. Hybrid nanorod-polymer solar cells. *Science* **2002**, *295*, 2425–2427.

[4] Xu, S.; Hansen, B. J.; Wang, Z. L. Piezoelectric-nanowire-enabled power source for driving wireless microelectronics. *Nat. Commun.* **2010**, *1*, 93.

[5] Wang, Z. L.; Song, J. H. Piezoelectric nanogenerators based on zinc oxide nanowire arrays. *Science* **2006**, *312*, 242–246.

[6] Wang, Z. L. Self-powered nanosensors and nanosystems. *Adv. Mater.* **2012**, *24*, 280–285.

[7] Sebald, G.; Lefeuvre, E.; Guyomar, D. Pyroelectric energy conversion: Optimization principles. *IEEE Trans. Ultrason. Ferroelectr. Freq. Control.* **2008**, *55*, 538–551.

[8] Yang, Y.; Jung, J. H.; Yun, B. K.; Zhang, F.; Pradel, K. C.; Guo, W. X.; Wang, Z. L. Flexible pyroelectric nanogenerators using a composite structure of lead-free $KNbO_3$ nanowires. *Adv. Mater.* **2012**, *24*, 5357–5362.

[9] Yang, Y.; Guo, W. X.; Pradel, K. C.; Zhu, G.; Zhou, Y. S.; Zhang, Y.; Hu, Y. F.; Lin, L.; Wang, Z. L. Pyroelectric nanogenerators for harvesting thermoelectric energy. *Nano Lett.* **2012**, *12*, 2833–2838.

[10] Beeby, S. P.; Torah, R. N.; Tudor, M. J.; Glynne-Jones, P.; O'Donnell, T.; Saha, C. R.; Roy, S. A micro electromagnetic generator for vibration energy harvesting. *J. Micromech. Microeng.* **2007**, *17*, 1257–1265.

[11] Park, J. C.; Park, J. Y. A bulk micromachined electromagnetic micro-power generator for an ambient vibration-energy-harvesting system. *J. Korean Phys. Soc.* **2011**, *58*, 1468–1473.

[12] Tang, W.; Meng, B.; Zhang, H. X. Investigation of power generation based on stacked triboelectric nanogenerator. *Nano Energy* **2013**, *2*, 1164–1171.

[13] Han, C. B.; Du, W. M.; Zhang, C.; Tang, W.; Zhang, L. M.; Wang, Z. L. Harvesting energy from automobile brake in

contact and non-contact mode by conjunction of tribo-electrication and electrostatic-induction processes. *Nano Energy* **2014**, *6*, 59–65.

[14] Xie, Y. N.; Wang, S. H.; Niu, S. M.; Lin, L.; Jing, Q. S.; Su, Y. J.; Wu, Z. Y.; Wang, Z. L. Multi-layered disk triboelectric nanogenerator for harvesting hydropower. *Nano Energy* **2014**, *6*, 129–136.

[15] Fan, F. R.; Tian, Z. Q.; Wang, Z. L. Flexible triboelectric generator. *Nano Energy* **2012**, *1*, 328–334.

[16] Yi, F.; Lin, L.; Niu, S. M.; Yang, J.; Wu, W. Z.; Wang, S. H.; Liao, Q. L.; Zhang, Y.; Wang, Z. L. Self-powered trajectory, velocity, and acceleration tracking of a moving object/body using a triboelectric sensor. *Adv. Funct. Mater.* **2014**, *24*, 7488–7494.

[17] Su, Y. J.; Zhu, G.; Yang, W. Q.; Yang, J.; Chen, J.; Jing, Q. S.; Wu, Z. M.; Jiang, Y. D.; Wang, Z. L. Triboelectric sensor for self-powered tracking of object motion inside tubing. *ACS Nano* **2014**, *8*, 3843–3850.

[18] Du, W.; Han, X.; Lin, L.; Chen, M.; Li, X.; Pan, C.; Wang, Z. L. A three dimensional multi-layered sliding triboelectric nanogenerator. *Adv. Energy Mater.* **2014**, *4,* 1301592.

[19] Zhong, J. W.; Zhang, Y.; Zhong, Q. Z.; Hu, Q. Y.; Hu, B.; Wang, Z. L.; Zhou, J. Fiber-based generator for wearable electronics and mobile medication. *ACS Nano* **2014**, *8*, 6273–6280.

[20] Jing, Q. S.; Zhu, G.; Wu, W. Z.; Bai, P.; Xie, Y. N.; Han, R. P. S.; Wang, Z. L. Self-powered triboelectric velocity sensor for dual-mode sensing of rectified linear and rotary motions. *Nano Energy* **2014**, *10*, 305–312.

[21] Wang, Z. L. Triboelectric nanogenerators as new energy technology for self-powered systems and as active mechanical and chemical sensors. *ACS Nano* **2013**, *7*, 9533–9557.

[22] Wang, S. H.; Lin, L.; Xie, Y. N.; Jing, Q. S.; Niu, S. M.; Wang, Z. L. Sliding-triboelectric nanogenerators based on in-plane charge-separation mechanism. *Nano Lett.* **2013**, *13*, 2226–2233.

[23] Niu, S. M.; Wang, S. H.; Lin, L.; Liu, Y.; Zhou, Y. S.; Hu, Y. F.; Wang, Z. L. Theoretical study of contact-mode triboelectric nanogenerators as an effective power source. *Energ. Environ. Sci.* **2013**, *6*, 3576–3583.